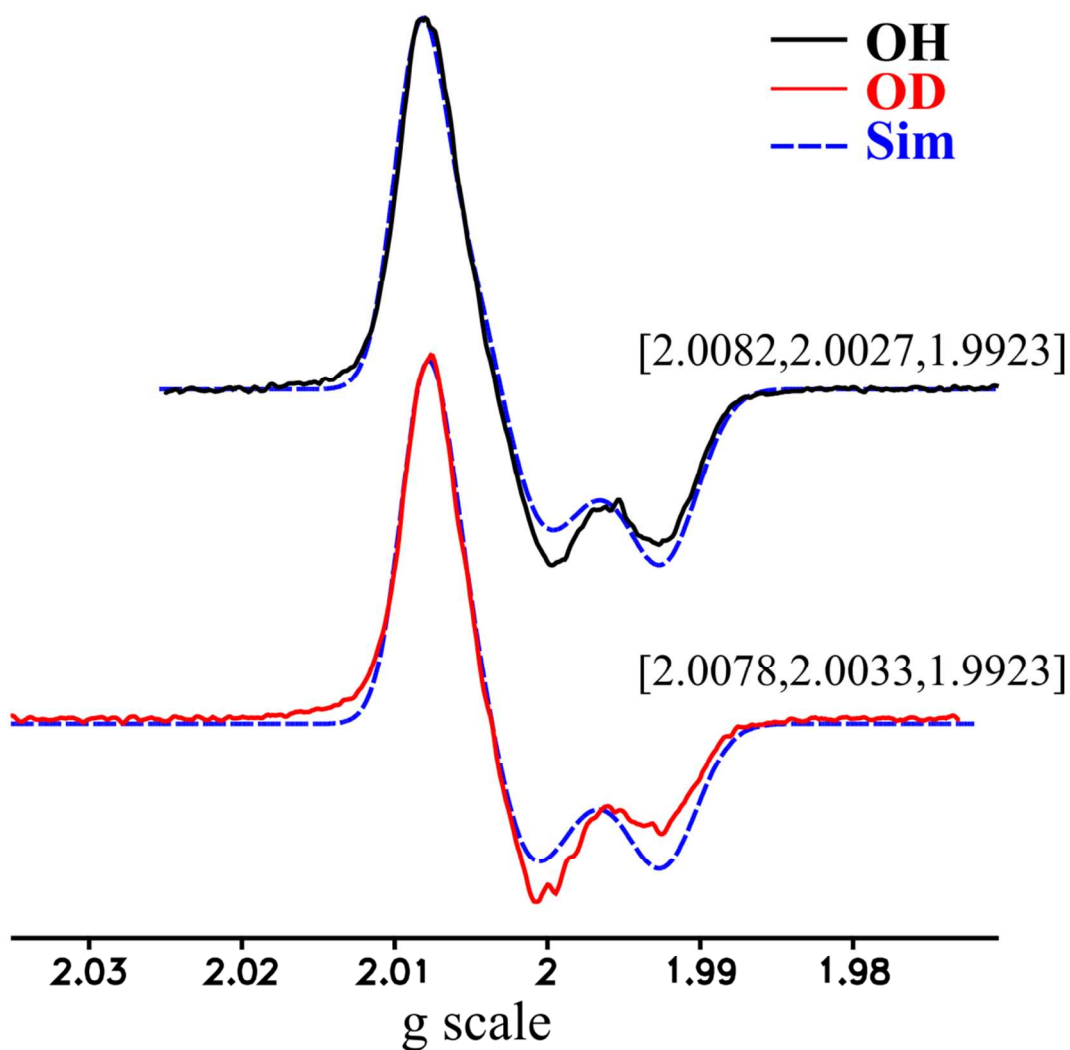


## Supporting Information for

# <sup>1</sup>H-ENDOR Evidence for a Hydrogen Bonding Interaction That Modulates the Reactivity of a Nonheme Fe<sup>IV</sup>=O Unit

Muralidharan Shanmugam,<sup>#</sup> Genqiang Xue,<sup>‡</sup> Lawrence Que Jr.,<sup>‡\*</sup> Brian M. Hoffman<sup>#\*</sup>

<sup>#</sup>Chemistry Department, Northwestern University, Evanston, Illinois, 60208-3113, <sup>‡</sup>Department of Chemistry  
and Center for Metals in Biocatalysis, University of Minnesota, Minneapolis, Minnesota-55455



**Fig S1: Solid lines:** Echo-detected 35 GHz EPR spectra of **1** in OH/OD. Derivative spectra generated by numerical derivatives of absorption-display spectra. **Dashed lines:** Simulations performed using WIN-EPR program; g-values for the fits are listed. *Conditions:* Two-pulse echo,  $\pi$ -pulse = 80 ns,  $\tau$  = 600 ns, repetition time = 50 ms, 34.698 GHz (OH), 34.75 GHz (OD), T = 2 K.

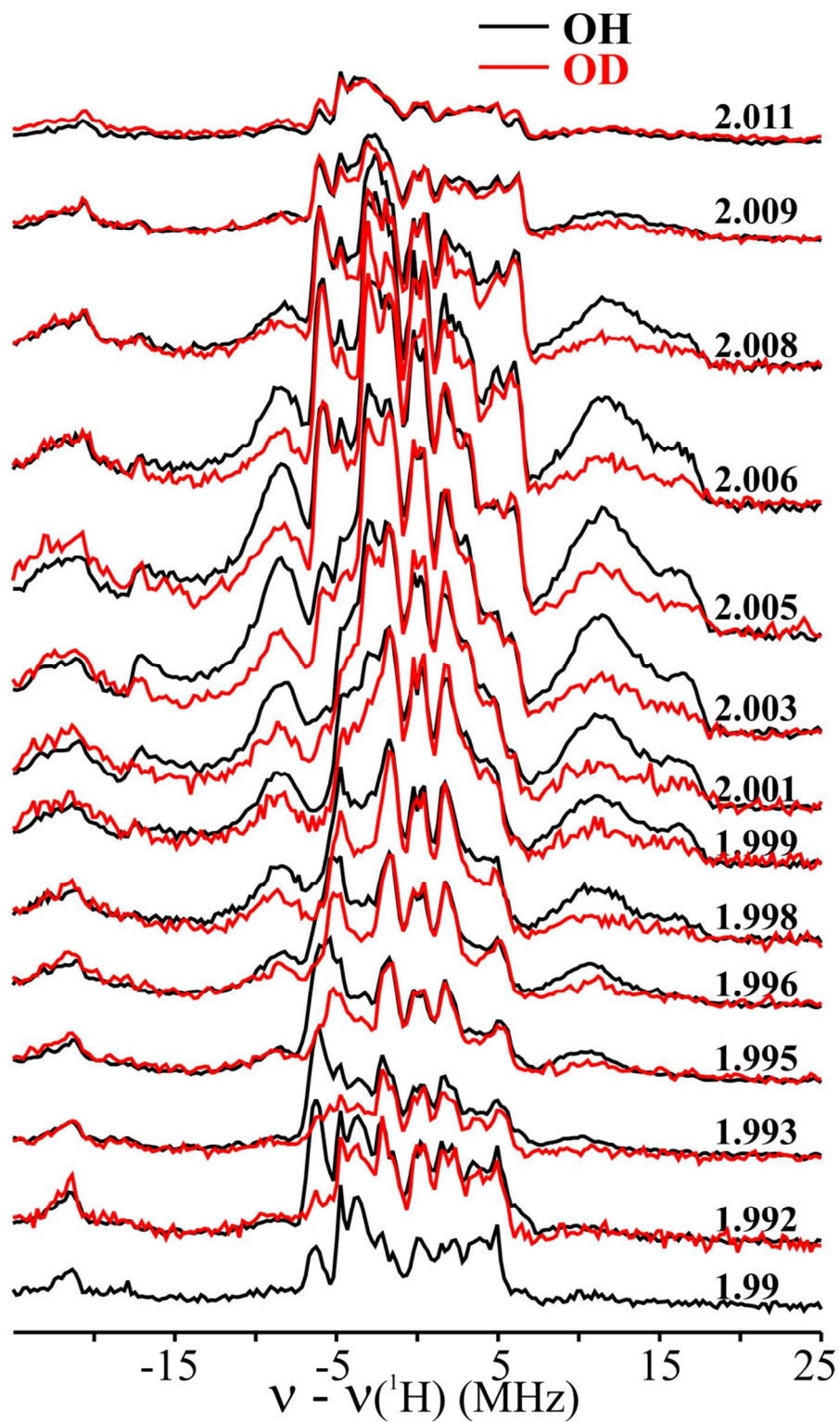


**Fig S2:** Experimental 2-D field-frequency plot of Davies  $^1\text{H}$ -ENDOR spectra of **1** in OH (black) and OD (red). All spectra have been centered at  $^1\text{H}$  nuclear Larmor frequency. *Conditions:*  $\pi$  pulse length = 120 ns,  $\tau$  = 600 ns, repetition time = 40 ms, 34.698 GHz (OH), 34.75 GHz (OD),  $T$  = 2 K.

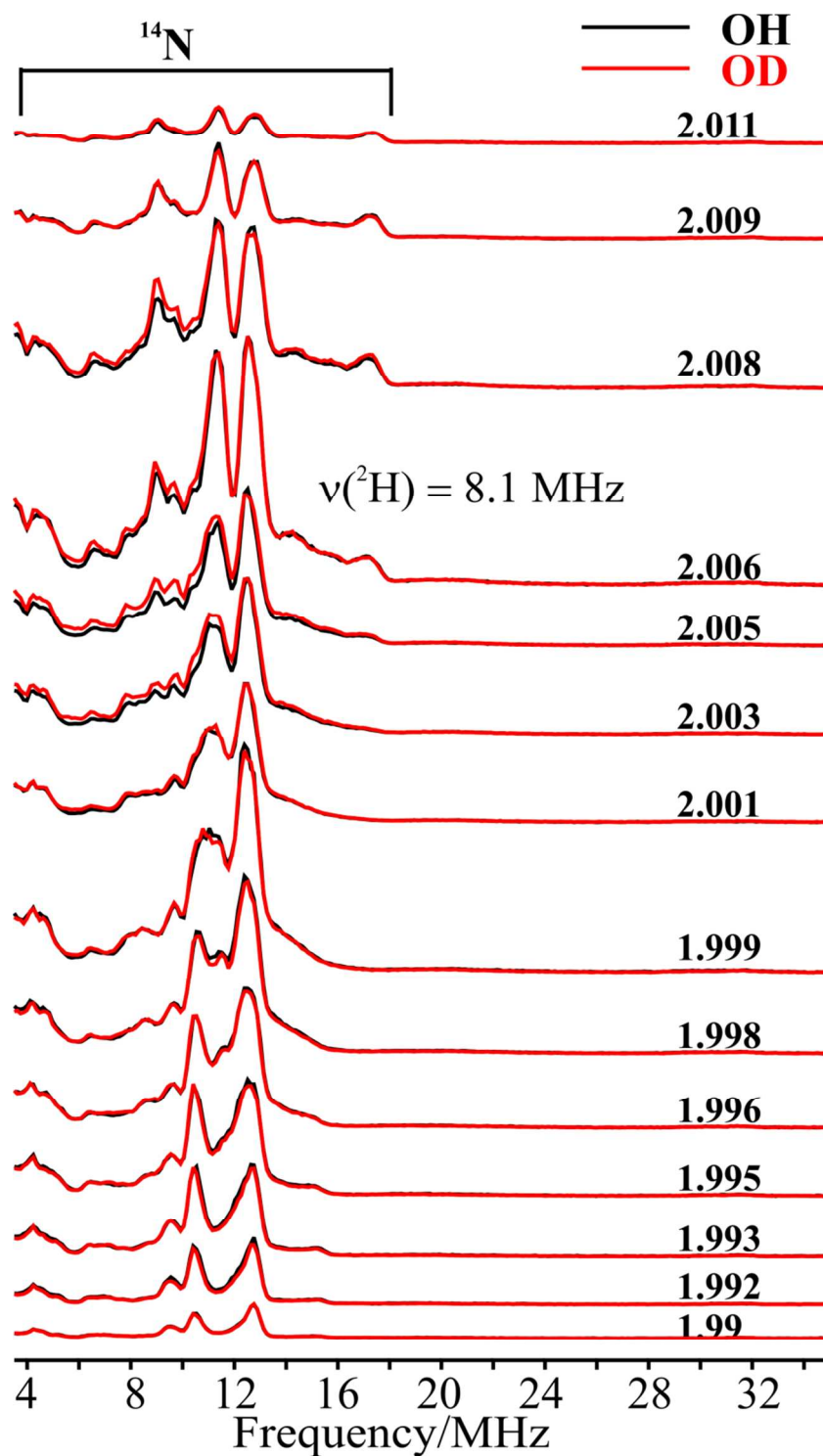


**Fig S3:** Experimental 2-D field-frequency plot of Davies  $^{14}\text{N}$ -ENDOR spectra of **1** in OH (black) and OD (red). *Conditions:*  $\pi$  pulse length = 120 ns,  $\tau$  = 600 ns, repetition time = 40 ms, 34.713 GHz (OH), 34.722 GHz (OD),  $T = 2 \text{ K}$ .

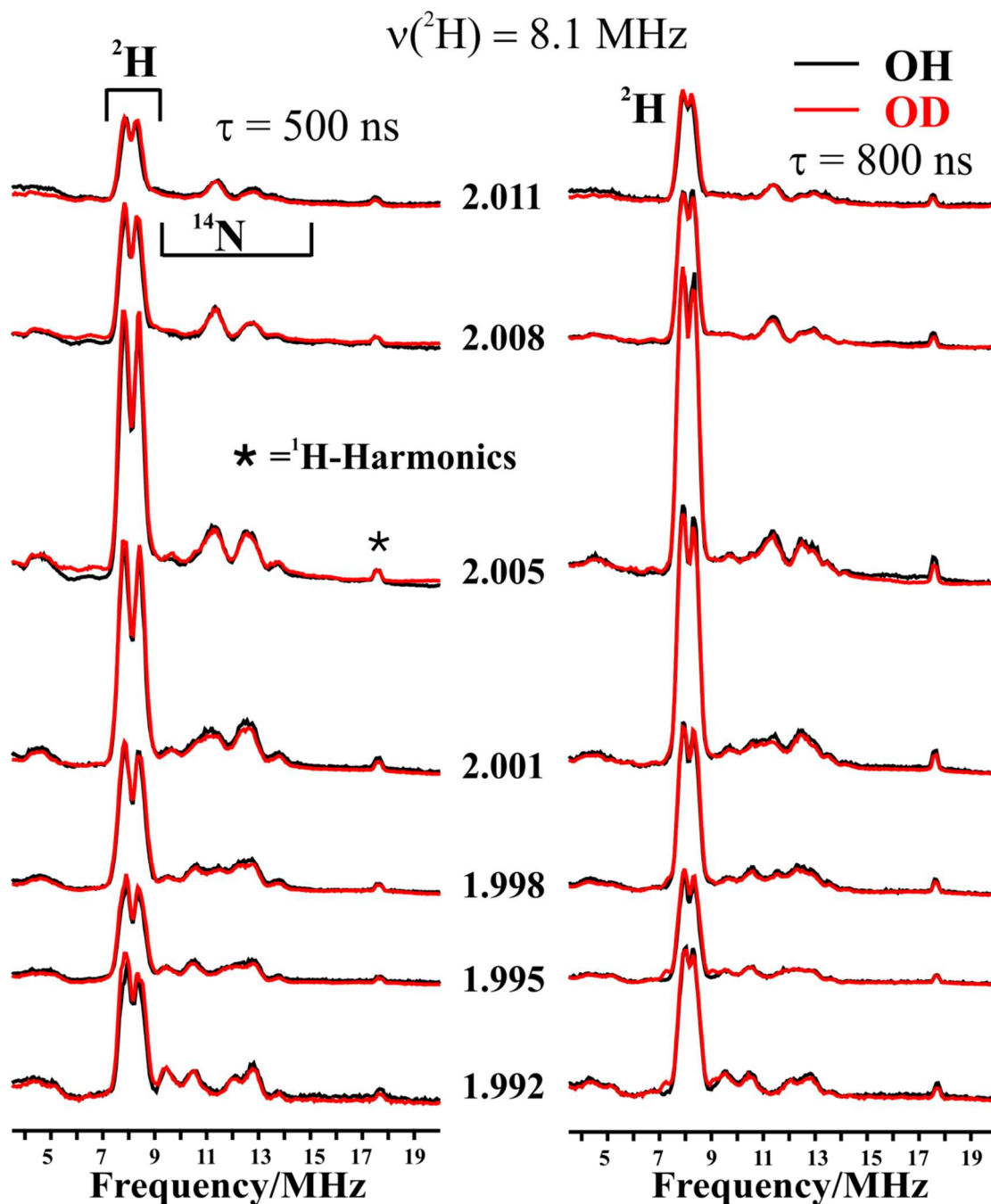


**Fig S4:** Experimental 2-D field-frequency plot of Mims  $^2\text{H}$  and  $^{14}\text{N}$ -ENDOR spectra of **1** in OH (black) and OD (red). The  $^2\text{H}$ -doublet centered at  $\nu_{\text{D}}$  arises from the deuterated methylene arms of **L** (Scheme 1). Conditions:  $\pi/2$  pulse length = 50 ns, repetition time = 40 ms, 34.713 GHz (OH), 34.722 GHz (OD), T = 2 K.

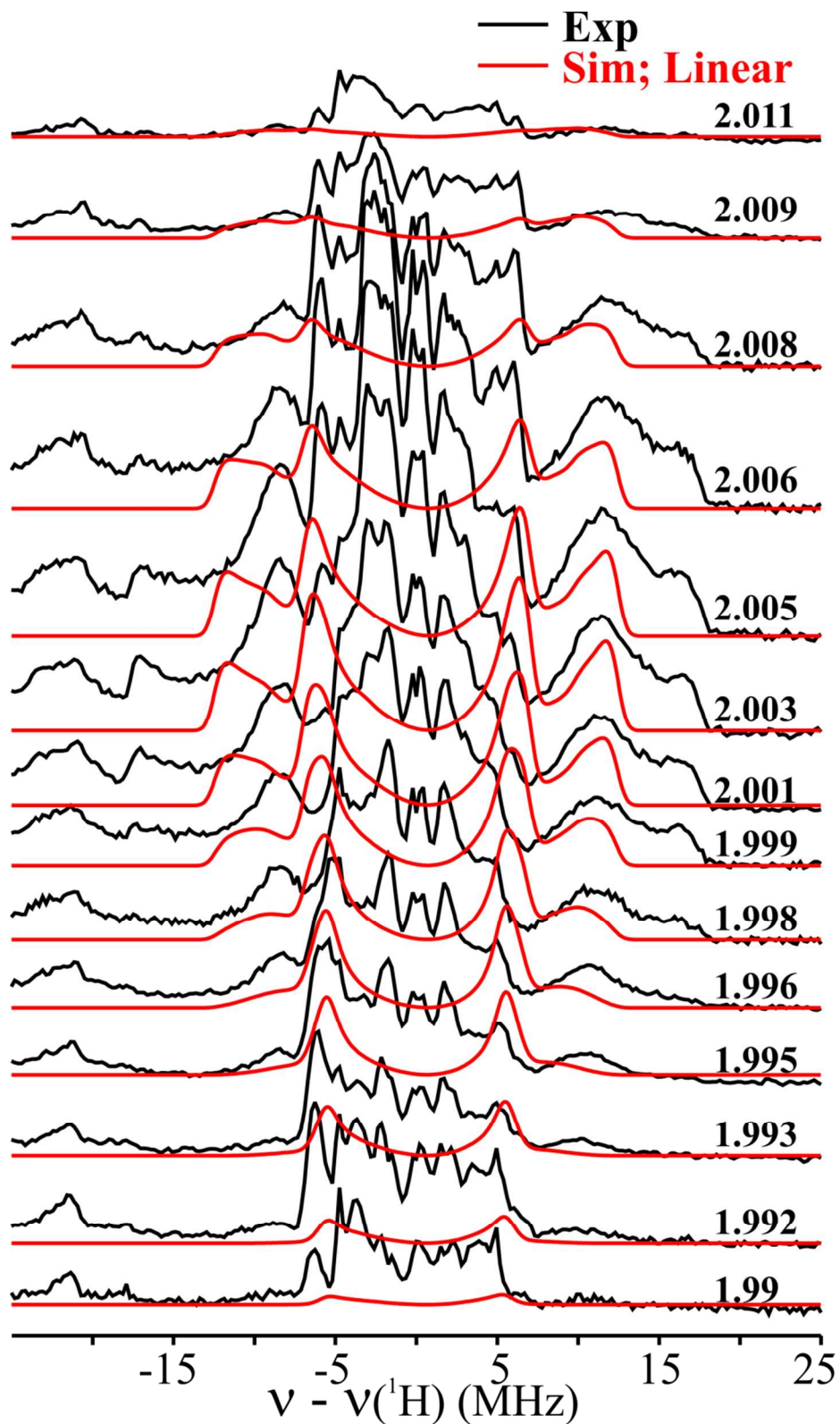


**Fig S5:** Comparisons of experimental 2-D  $^1\text{H}$ -ENDOR pattern of **1(OH)** with simulation performed by assuming a linear  $\text{Fe(III)}-\mu(\text{O})-\text{Fe(IV)}$  geometry. The metrical and Spin-Hamiltonian parameters used to do the simulation are given in table S1.

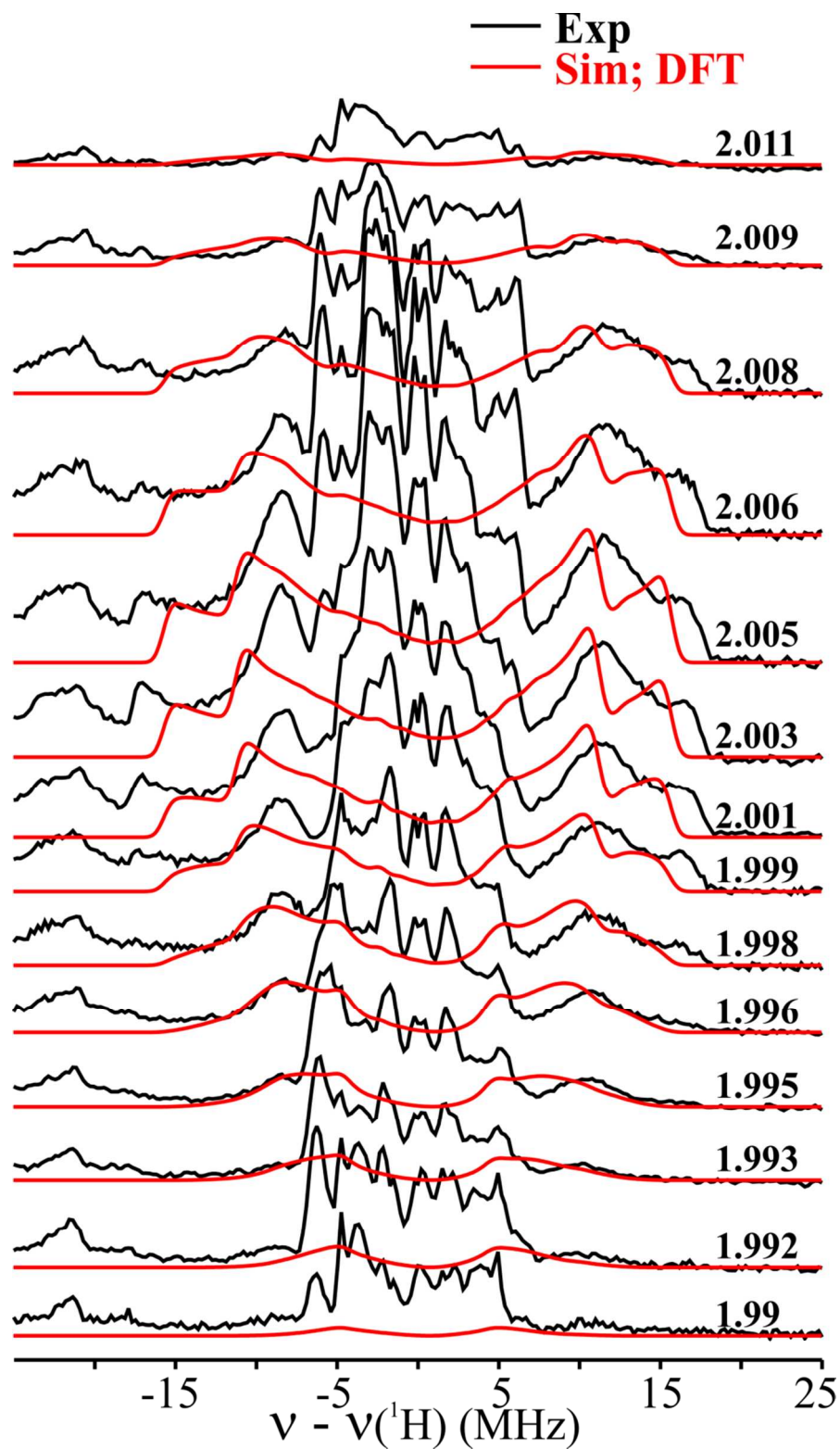


**Fig S6:** Comparisons of experimental 2-D  $^1\text{H}$ -ENDOR pattern of  $\mathbf{1(OH)}$  with simulation performed by assuming DFT optimized location of  $^1\text{H}_A$ , whose metrical and Spin-Hamiltonian parameters are given in table S1.

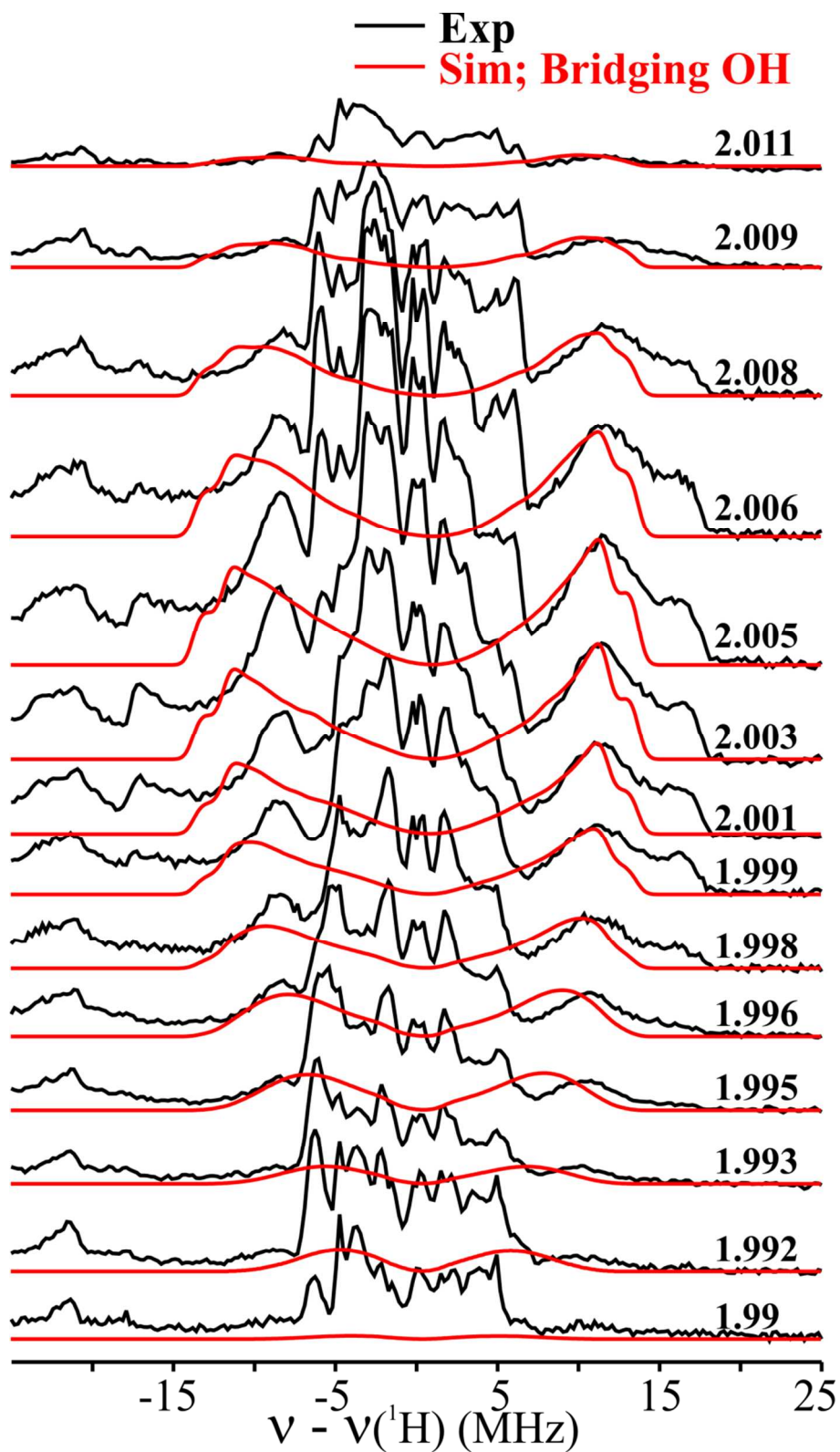


**Fig S7:** Comparisons of experimental 2-D  $^1\text{H}$ -ENDOR pattern of  $1(\text{OH})$  with simulation performed by assuming a bridging  $\mu(\text{OH})$  hydroxide, by adding to proton to a  $\mu(\text{O})$  bridge, whose metrical and Spin-Hamiltonian parameters are given in table S1.

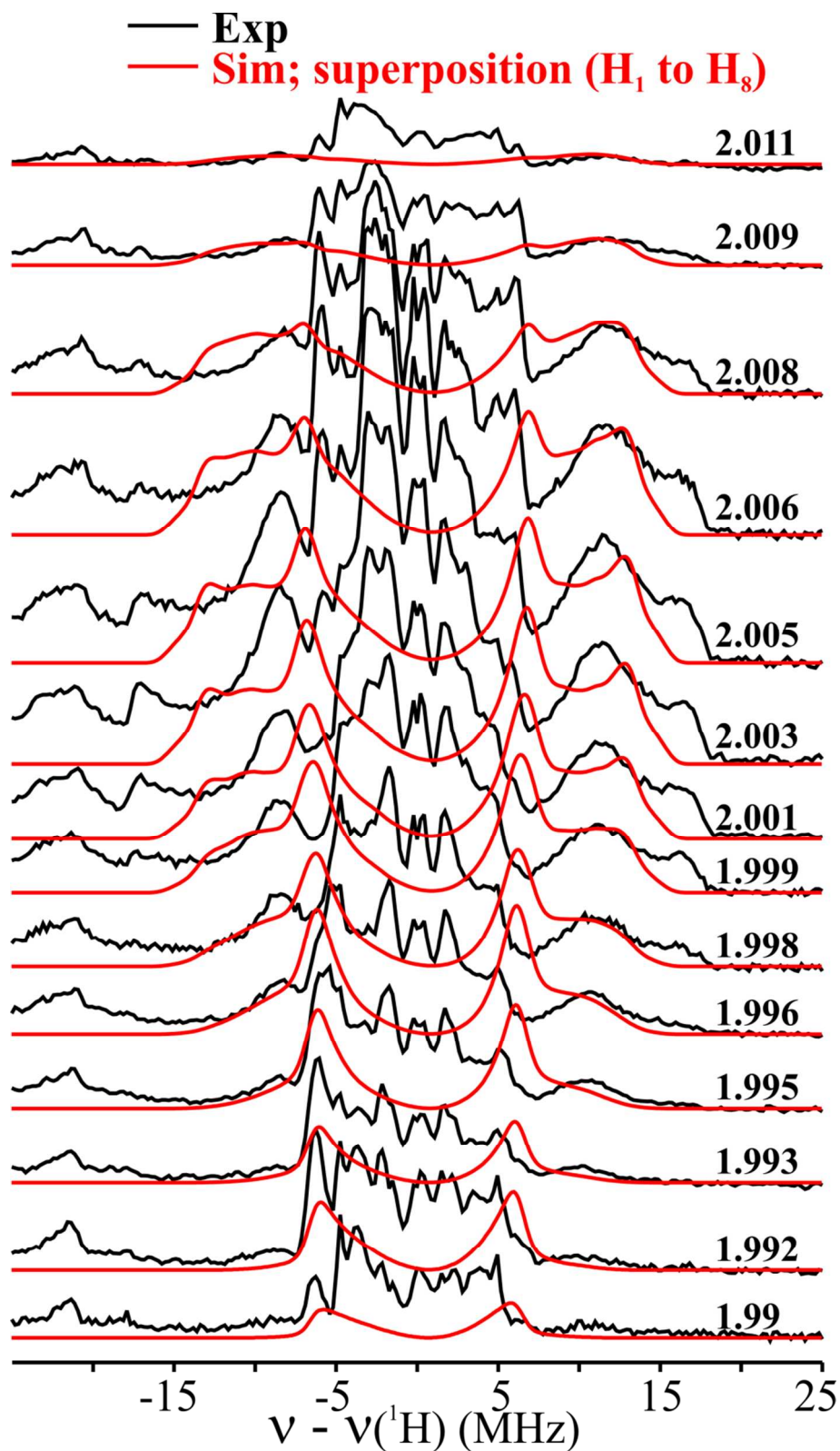


**Fig S8:** Comparisons of experimental 2-D  $^1\text{H}$ -ENDOR pattern of **1(OH)** with simulation performed by assuming  $^1\text{H}_A$  to be randomly rotated around the Fe(III)-O bond, with the superposition 2-D spectra obtained by summing the simulations, corresponding to multiple  $^1\text{H}_A$  orientations whose metrical and dipolar tensors are given in table S2.



**Table S1:** Metrical and  $^1\text{H}$  Spin-Hamiltonian Parameters used to simulate 2-D pattern for  $^1\text{H}_\text{A}$ 

Metrical Parameters	Experiment <sup>a</sup>		$^1\text{H}_\text{A}$ Hyperfine tensors			
	$\mathbf{A}_\text{exp}$	$\mathbf{T}_\text{exp}$	$\mathbf{T}$ : Modified DFT <sup>b</sup>	$\mathbf{T}$ : Linear <sup>c</sup> geometry	$\mathbf{T}$ : DFT <sup>d</sup>	$\mathbf{T}$ : Bridging <sup>e</sup> OH
$A_1/T_1$ (MHz)	-25	-24.3	-24.3	-14.0	-22.4	-23.7
$A_2/T_2$ (MHz)	-12	-11.3	-11.3	-10.9	-9.0	-3.7
$A_3/T_3$ (MHz)	34.8	+35.6	+35.6	+24.9	+31.4	+27.4
$a_\text{iso}$ (MHz)	-	0	0	0	0	0
$\lambda = (T_2 - T_1)/T_3$	0.73	0.365	0.365	0.126	0.427	0.73
$d_{\text{Fe-Fe}}$ (Å)				3.7	3.341	3.341
$r_1$ (Å)			<b>2.198</b>	<b>2.387</b>	<b>2.387</b>	<b>2.52</b>
$(\beta_1)$ (deg)			<b>53.8</b>	<b>80.6</b>	<b>56.6</b>	<b>44.4</b>
$\gamma$ (deg)				78.4	53.8	43.1
$r_2$ (Å)				4.1	2.843	2.341
$(\beta_2)$ (deg)				144.5	135.5	131.1

<sup>a</sup> Tensor used in simulations of experiment, **Figure 2**, using  $\mathbf{g} = [2.008, 2.003, 1.992]$ .

<sup>b</sup> Tensor calculated using Fe-Fe distance from DFT optimized geometry<sup>1</sup> with slightly repositioned  $^1\text{H}_\text{A}$  exactly matches  $\mathbf{T}$  derived from experiment.

<sup>c</sup> Tensor calculated using metrical parameters of DFT optimized<sup>1</sup> geometry of **1** as modified by linearizing the Fe-O-Fe fragment. Simulations with this tensor, **Figure S5** do not match.

<sup>d</sup> Tensor calculated using metrical parameters of DFT optimized<sup>1</sup> geometry of **1**; simulations with this tensor, **Figure S6** do not match.

<sup>e</sup> Tensor calculated using metrical parameters of DFT optimized<sup>1</sup> geometry of **1** as modified by adding a proton to a  $\mu(\text{O})$ -bridge. Simulations with this tensor, **Figure S7**, do not match.

**Table S2:** Metrical and  $^1\text{H}$  Spin-Hamiltonian Parameters used to simulate the superposition 2-D  $^1\text{H}$ -ENDOR pattern displayed in Figure S8.

Metrical Parameters	DFT Optimized geometry for X-Model							
	H <sub>1</sub> (DFT)	H <sub>2</sub> (+45°)	H <sub>3</sub> (-44°)	H <sub>4</sub> (+89°)	H <sub>5</sub> (-87°)	H <sub>6</sub> (+124°)	H <sub>7</sub> (-121°)	H <sub>8</sub> (+141°)
$A_1/T_1$ (MHz)	-22.4	-18.6	-20.5	-15.5	-16.6	-14.5	-14.9	-14.3
$A_2/T_2$ (MHz)	-9.0	-10.6	-9.8	-11.9	-11.4	-12.3	-12.2	-12.4
$A_3/T_3$ (MHz)	+31.4	+29.2	+30.3	+27.4	+28.0	+26.8	+27.1	+26.7
$a_{\text{iso}}$ (MHz)	0	0	0	0	0	0	0	0
$\lambda = (T_2 - T_1)/T_3$	0.427	0.274	0.353	0.131	0.186	0.082	0.10	0.071
$d_{\text{Fe-Fe}}$ (Å)	3.341							
$r_1$ (Å)	2.387							
$(\beta_1)$ (deg)	<b>56.6</b>	<b>68.0</b>	<b>61.3</b>	<b>86.5</b>	<b>77.7</b>	<b>99.4</b>	<b>93.1</b>	<b>102.3</b>
$\gamma$ (deg)	53.8	64.6	58.1	83.4	74.4	83.1	89.7	80.1
$r_2$ (Å)	2.843	3.3	3.0	4.0	3.7	4.4	4.2	4.5
$(\beta_2)$ (deg)	135.5	137.9	136.3	143.3	140.5	147.7	145.5	148.8

**References:**

- (1) De Hont, R. F.; Xue, G.; Hendrich, M. P.; Que, L.; Bominaar, E. L.; Munck, E. *Inorg. Chem.* **2010**, *49*, 8310-8322.